Research paper

Study of temperature field in large-span steel structure under radiation-thermal-fluid coupling

Pengcheng Jiang[1]

Abstract: The non-uniformity of temperature field distribution of long-span steel structure is proportional to the intensity of solar radiation. Based on the background of Guangzhou Baiyun Station large-span complex steel roof structure, this paper studies the non-uniform temperature field distribution of large-span steel structure under the Summer Solstice daily radiation-thermal-fluid coupling action based on Star-ccm+ finite element software, and uses Spa2000 software to analyze the stress and deformation of steel roof under temperature action. Combined with the on-site temperature monitoring, the maximum difference with the measured value is 2.5°C compared with the numerical simulation results, which verifies the validity of the finite element simulation. The results show that: from 8:00, with the increase of solar altitude angle, the intensity of solar radiation increases, the temperature rises, and the temperature distribution of large-span steel structure becomes more and more non-uniform. From 14:00 to 18:00, the solar radiation weakens, and the temperature distribution tends to be uniform. Finally, reasonable construction suggestions and measures are proposed to reduce the adverse effects of temperature effects, which can provide theoretical references for the safe construction and normal operation of large-span steel structures located in the subtropics.

Keywords: large-span steel structure, temperature effect, non-uniform temperature field, thermal radiation

[1]Eng., Station Construction Command, China Railway Guangzhou Group Co., Ltd., Guangzhou, Guangdong, China, e-mail: gzjzfz@163.com, ORCID: 0000-0003-4321-5952

1. Introduction

With the advantages of light weight and high strength materials and good seismic resistance, large span steel structures are being used in more and more public buildings to meet the needs of large spaces and structural aesthetics. Under strong sunlight, the surface temperature of large-span steel structures is much higher than the atmospheric temperature, which generates transient inhomogeneous temperature fields in the steel structure and changes continuously with time. In addition, the variable temperature and restraint can cause large thermal deformation in large-span steel structures, and if not properly resolved, the temperature stresses can cause excessive rod displacement, increased bearing reactions and steel structure strength degradation [1].

There have been some researches on the effect of temperature on steel structures at home and abroad. P. Woźniczka [2] estimated the non-uniform fire temperature distribution of long-span steel truss girders by analyzing different fire scenarios. G. Flint et al. [3] studied the deformation and stresses of a truss structure under the effect of temperature by using of finite element analysis software simulations with different constraints and heating conditions. Kallada Janardhan Rahul [4] studied the response of a large-span steel truss beam under a non-uniform temperature field based on a computational fluid dynamics fire simulation and finite element analysis combined with a unidirectional coupling method. A study by Lenka Lausova [5] showed that in super-stationary structures, a non-uniform temperature field caused additional bending moments. Liu et al. [6] conducted field experiments and finite element simulations on large-span glass roofs and light roofs exposed to sunlight, and proposed that an increase in temperature was the primary factor affecting member stress and a decrease in temperature was the primary factor affecting node displacement. Xu [7] established a numerical simulation approach for the temperature field of a space truss structure considering instantaneous shadow effect to study the steel roof of the Xi'an Silk Road International Convention and Exhibition Center, concluded that the detrimental effect of non-uniform temperature field on the structural performance was notable and the solar radiation intensity was positively related to the temperature field inhomogeneity. Liu [8] used the Sap2000 software to analyze the temperature stresses in the large-span steel roof of the Shanghai National Convention and Exhibition Center, and then proposed three methods that could reduce the temperature stresses by combining the characteristics of the trusses. Fan et al. [9] obtained the solar radiation intensity of the components in each area of the saddle-shaped hyperbolic large-span roofs of the National Stadium by analyzing statistics, determined the parameters and boundary conditions required for the finite element calculation of the temperature field, and determined the closing temperature and construction requirements of the large-span roof structure based on the calculation results. At present, there are few studies that have analyzed the non-uniform temperature field in large-span steel structures with "grid + truss" combined roofs. Large-span steel structures are often located in places where a large number of people gather, and once structural damage occurs due to temperature effects or other superimposed loads, unpredictable losses can occur. When the racecourse of the 2010 Ordos International

Nadam Games experienced a sudden drop in temperature, the large telescopic deformation of the main steel structure with construction defects caused the collapse of the racecourse [10].

In this paper, the large-span steel roof of the Baiyun Station in Guangzhou, China, is used as the research object, and the non-uniform temperature field is analyzed using numerical simulations and field monitoring. At the same time, reasonable construction suggestions and measures are proposed to reduce the adverse effects of temperature action, which have engineering significance to ensure the safe construction and normal operation of large-span steel structures located in the subtropics.

2. Basic theoretical approach

Steel structures exposed to sun in natural environment experience two types of radiation, long-wave radiation and short-wave radiation. Long-wave radiation is the radiation heat exchange between the earth and gas, and short-wave radiation is direct, reflected, and scattered radiation. There are three basic types of heat exchange between the interior and the surface of a steel structure: thermal convection, heat conduction, and thermal radiation. Thermal convection is the exchange of heat that occurs in a fluid due to a temperature difference. It follows Newton's law, where the airflow near a hot object expands with heat, decreases in density and moves upward, and the colder air with higher density moves downward to replace the original heat flow position. Heat conduction involves a large number of molecular thermal movements in a solid, such that energy is transferred from a high temperature area of an object to a low temperature area, following Fourier's law. When sun shines on a steel structure, there is always a part of the structure in the shadow part, where the temperature is lower than the part exposed to the sun. Heat conduction and thermal convection often occur simultaneously, making the temperature change with complex time variability. Thermal radiation refers to the process in which an object emits energy in the form of electromagnetic waves outward because it has a certain temperature of its own. All objects with a temperature above absolute zero can generate thermal radiation, and the higher the temperature, the stronger the thermal radiation. Under sunlight, the air and a steel structure are heated, thermal radiation is enhanced between the air and the structure, which have different heat capacities, resulting in a temperature gradient, and heat transfer. With the flow of air, convective heat transfer continues, so that under the sun's irradiation, radiation, heat flow, and fluid coupling forms between the physical fields. The sunlight radiation mechanism is shown in Fig. 1.

The solar radiation calculation models are the Dilger model, the Hottel model, and the ASHRAE clear-sky model [11]. In this paper, the Star-ccm+ software is used to analyze the non-uniform temperature field of Baiyun station's "grid + truss" roof of under the action of radiation-thermal-fluid coupling, in which the solar radiation calculation is based on the ASHRAE clear sky model, which is commonly used in the field of structural engineering. In the ASHRAE model, solar radiation consists of direct radiation, reflected radiation from the ground surface, and scattered radiation from the sky as follows:
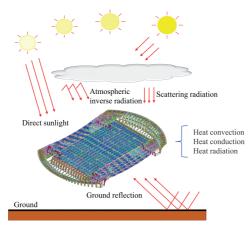
Fig. 1. Sunlight radiation mechanism

1. Direct solar radiation intensity

$$(2.1) \qquad G_{ND} = \frac{A}{\exp\left(\dfrac{B}{\sin\beta}\right)} C_N$$

$$(2.2) \qquad G_D = G_{ND} \cos(\theta)$$

where G_{ND} is the direct radiation intensity, W/m^2; G_D is the direct radiation intensity received by the surface of the component, W/m^2; A is the radiation intensity when the atmospheric mass is equal to zero, W/m^2; B is the extinction coefficient; C_N is the atmospheric cleanliness; β is the solar altitude angle; θ is the incident inclination angle.

2. Sky scattered radiation intensity

The formula for calculating the intensity of scattered radiation from a cloud-free non-vertical surface in a clear sky is

$$(2.3) \qquad G_{d\theta} = CG_{ND}\left(\frac{1+\cos\alpha}{2}\right)$$

where C is the ratio of scattered radiation to vertical incident radiation and α is the angle of incidence.

The formula for calculating the intensity of scattered radiation from a cloud-free vertical surface in a clear sky is

$$(2.4) \qquad G_{d\theta} = \frac{G_{dV}}{G_{dH}} CG_{ND}$$

$$(2.5) \qquad \frac{G_{dV}}{G_{dH}} = \begin{cases} 0.55 + 0.437\cos\theta + 0.313\cos^2\theta & \cos\theta > -0.2 \\ 0.45 & \cos\theta \le -0.2 \end{cases}$$

where G_{dV} is the incident scattered radiation in the vertical plane on a clear day and G_{dH} is the incident scattered radiation in the horizontal plane on a clear day; θ is the incident inclination angle.

3. The surface of ground reflected radiation intensity

$$(2.6) \qquad G_R = G_{tH} \rho_g \frac{1 - \cos \alpha}{2}$$

where: G_{tH} is the total radiation (direct + scattered), W/m^2; ρ_g is the horizontal surface or ground radiation reflectance.

3. Field measurements

3.1. Project overview

The Baiyun Station is located in the south of Baiyun District, Guangzhou City, and is one of the largest integrated hubs of railway stations in Asia. The station is located in the subtropics, south of the Tropic of Cancer, with a subtropical monsoon climate, and receives high heat from sun exposure. The annual average temperature is 21.8° and the annual average relative humidity is about 80%. January is the coldest month, whose an average temperature is 11.2°; July is the hottest month, whose an average temperature is 28.8°, the historical extreme temperatures are –1.9° and 38.5°, respectively. The temperature change from 2020 to 2021 is plotted based on the weather station data in Baiyun District, Guangzhou, as shown in Fig. 4.

The roof of the central waiting room of the Baiyun Station adopts a wavy "ribbon" design on the north and south sides formed of a space triangle steel pipe grid + truss frame structure combination with spherical seismic steel bearings. The truss structure is shown in Fig. 2, and the grid structure is shown in Fig. 3. The maximum span of the truss is 64 m, the maximum diameter of the steel pipe is 600 mm, the material is mainly Q355B and Q390B, the surface is coated with fireproof anti-corrosion, the primer is water-based inorganic zinc-rich primer, the intermediate paint is epoxy cloud iron intermediate paint, the top paint is fluorocarbon top coat. The projected area of the roof of the Baiyun station is 95,224 m^2, and the maximum dimension of the plan projection is 252.5 × 412 m. A total of 145 days (from 5 February, 2022 to 30 June, 2022) was required for the construction of
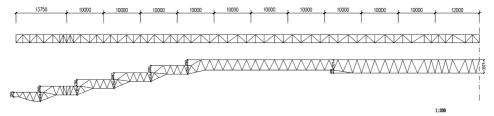

Fig. 2. Truss

the first phase roof. The The view of the steel roof is shown in Fig. 5. The properties of Q355B are shown in Table 1.
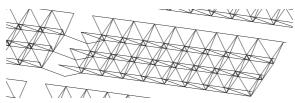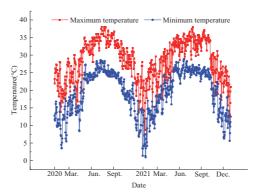

Fig. 3. Grid

Fig. 4. Daily temperature extremes from 2020 to 2021

Fig. 5. The view of the steel roof

Table 1. Physical properties of Q355B steel

Density (kg/m^3)	Modulus of elasticity (MPa)	Poisson's ratio	Linear thermal expansion coefficient (1/°C)	Yield strength (MPa)	Thermal conductivity (W/(m·K))	Solar radiation absorptivity
7850	2.0×10^5	0.3	1.2×10^{-5}	355	46	0.7

3.2. Measurement results

The summer solstice day, 21 June 2022, was designated as the experimental day, which the day was cloudy and sunny. The ambient temperature was measured using a dual-use temperature and humidity meter about 10m from the roof, as shown in the upper right corner of Fig. 6. The temperature measuring points are shown in Fig. 7, and there are 76 measurement points, all of which are arranged at the web members of the truss and grid. The temperature measurement area is divided into three areas I, II, and III, as shown in Fig. 8. The infrared thermal imager was used to measure the temperature of multiple measurement points of the grid + truss frame at six timepoints: 8:00, 10:00, 12:00, 14:00, 16:00, and 18:00; the average value of temperature in spatial sense was taken as the final result. The Hikvision K20 thermal imager has a visual temperature measurement function with a temperature measurement range of $-20 \div 400°$ and an accuracy of $\pm 2°$, as shown in the upper left corner of Fig. 6. The field measurements are shown in Fig. 6, and the temperature measurement data are shown in Table 2.
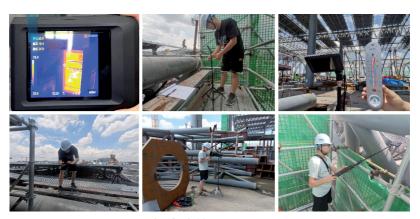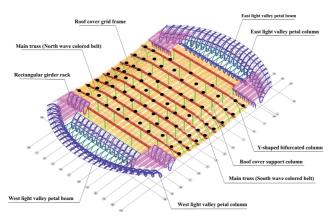

Fig. 6. Field measurement
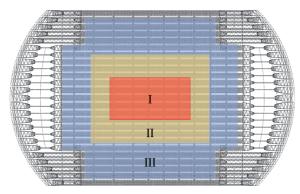

Fig. 7. Distribution of measurement points

Fig. 8. Temperature measurement area

Table 2. Temperature measurement results

Time	Ambient temperature (°)	Average temperature of zone I (°)	Average temperature of zone II (°)	Average temperature of zone III (°)
8:00	28.0	39.9	38.4	36.3
10:00	29.4	41.8	40.6	39.4
12:00	30.2	43.2	42.2	41.5
14:00	30.5	49.7	45.3	43.1
16:00	29.8	45.8	43.4	41.2
18:00	28.8	42.6	40.8	38.1

Influenced by solar radiation, ambient temperature and flow field changes, the temperature of the steel roof cover trends in the same direction as the ambient temperature. From the temperature measurement results, it can be seen that the average temperature of the steel roof surface is greater than the ambient temperature, and zone I > zone II > zone III. The lowest value of temperature measurement appeared in zone III at 8:00 am with a temperature of 36.3°C. Due to the solar radiation, the peak value of 48.7°C was reached in zone I at 14:00, which was 18.2°C higher than the ambient temperature. Meanwhile, the unevenness reaches its highest level at 14:00, with a difference of 6.6°C between zone I and III. As time passes, the solar radiation weakens and the temperature begins to drop, completing a cycle of temperature rise and temperature fall.

4. Finite element analysis

Since the CAD 3D model is composed of lines, the effect of temperature distribution simulation is not ideal, so the line element is transformed into surface element [6], and the simplified model of steel roof truss + grid is established in the software Star-ccm+, as

shown in Fig. 9. To simulate the temperature field distribution of the large-span steel roof at six timepoints, i.e., 8:00, 10:00, 12:00, 14:00, 16:00 and 18:00 on a summer solstice day, the solar calculator in the Star-ccm+ software was used to input the longitude and latitude of Baiyun District, Guangzhou, i.e., 23.883°N and 113.517°E, the date, and the timepoints. In order to ensure the accuracy of the numerical simulation, the software calculation takes into consideration the shading effect between the components and the flow field effect. The inlet fluid velocity is taken as the measured wind speed of 3.28 m/s at the weather station on the day, and the turbulence intensity is 0.01. The inlet fluid temperature is taken as the ambient temperature. The outlet is a pressure outlet with a pressure value of 1 atm. The turbulence intensity is taken as 0.01 and the outlet fluid temperature is taken as the ambient temperature. The relaxation factor is 0.3 and the implicit solution method is used. Because the temperature of the zone I of the steel roof is the highest, the infrared thermal imager was used to measure the temperature at the center of I zone to verify the simulation results. The simulation results and the thermal imaging results are shown in Fig. 10, where the "Cen" is the center of the temperature measurement images, and the "Min" temperature measurement points are located in the sky, so they are not included in the temperature measurement results. The simulated temperature maxima at different moments and the measured temperature maxima at the center of zone I are shown in Table 3.
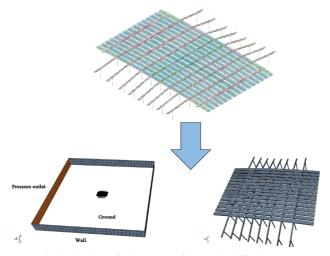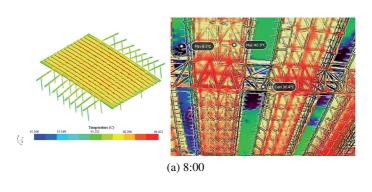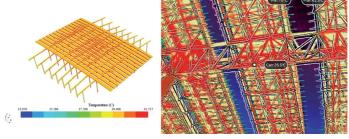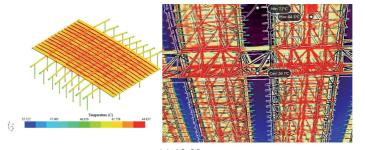

Fig. 9. Steel roof grid + truss frame simplified model

In Fig. 10, it can be seen that the highest temperature of the steel roof appears after the strongest moment of solar radiation, around 14:00, when the temperature difference also reaches the maximum, while the temperature field inhomogeneity is proportional to the intensity of solar radiation. At 10:00 when the temperature field distribution has a trend of inhomogeneity, with an increase in solar altitude angle, the solar radiation is enhanced, the temperature rises, and the temperature field inhomogeneity increases. Despite the maximum solar altitude angle at 12:00, the steel roof temperature does not reach its peak
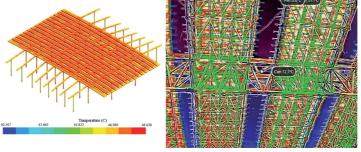
(a) 8:00

(b) 10:00

(c) 12:00

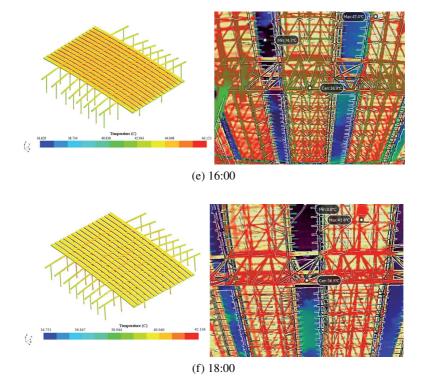(d) 14:00

(e) 16:00

(f) 18:00

Fig. 10. Simulated temperature and measured temperature in the center of zone I

Table 3. Maximum values of simulated and measured temperatures at different moments

Time	Simulated temperature maximum (°)	Maximum measured temperature in the center of zone I (°)
8:00	40.4	40.9
10:00	41.5	42.5
12:00	44.8	44.5
14:00	48.6	51.1
16:00	46.2	47.4
18:00	42.1	43.8

because the temperature increase caused by direct solar radiation takes some time, and after a period of heat accumulation, the temperature simulation results reaches its peak of 48.6°C at 14:00. This time-varying temperature effect causes significant non-uniform temperature deformation [12]. The stress and deformation displacement of the steel roof

reaching 48.6°C were simulated by using the software Sap2000, in Fig. 11 and 12. The results show that the steel structure is subjected to thermal expansion and is in a compressed state due to restraint [13], and the stress reaches $80 \div 120$ MPa and the displacement reaches its maximum value of 28.6 mm in zone I. The deformation displacement in zones II and III decreases sequentially. Since the roof supports are all fixed hinge supports, the temperature stress generated during the warming process of the structure cannot be released, so it is necessary to release the temperature stress of the structure and improve the safety of the structure in the actual project. In the construction of this project, we should focus on the deformation of steel structure in zone I. Heat insulation paint is used on the surface of the steel pipe to reduce the influence of temperature on the structure, and light-colored finish paint with small solar radiation absorption coefficient and strong infrared reflection ability should be selected, and movable hinge support is set to release part of the temperature deformation.
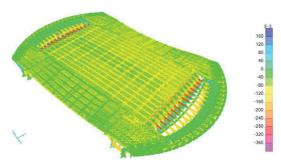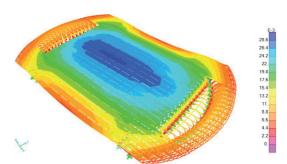

Fig. 11. Stress nephogram

Fig. 12. Displacement nephogram

From 14:00 to 18:00, the solar radiation weakened and the temperature distribution of the steel structure was gradually uniform. The simulation results from 8:00 to 18:00 show that the temperatures at the edges of the steel structure in zone III are all lower than the temperatures in the rest of the zone. The reason for the above phenomenon is that the members are far away from each other and the influence of heat radiation and heat

conduction between them is weak. From Table 3 and Fig. 10, the temperature simulation maximum value is similar to the measured temperature maximum value in the center of zone I, with a maximum difference of 2.5°C, which indicates the validity of the numerical simulation of the temperature field.

5. Conclusions

In this paper, the non-uniform temperature field of a steel roof grid + truss structure is investigated by means of numerical simulation and onsite monitoring. The following conclusions were drawn:

1. Under the action of solar radiation-thermal-fluid coupling, the temperature field of steel structure is non-uniform in proportion to the intensity of solar radiation. The steel structure temperature field from 10:00 to 14:00 is non-uniformly distributed, and the temperature reaches a peak at 14:00, which can reach 51.1°C, with a difference of 20.6°C from the ambient temperature. The rest of the time the solar radiation weakens, the temperature decreases, and the steel structure temperature distribution field tends to be uniform.

2. The simulated maximum temperature reached 48.6°C. At this temperature, the maximum deformation of the steel roof reached 28.8 mm and the stress reached $80 \div 120$ MPa.

3. As the temperature rises, the temperature stresses also accumulate and increase. Therefore, the temperature stress of the steel structure should be released during the construction process to reduce the temperature deformation and stress generated by the non-uniform temperature field of the steel structure and to improve the safety of the structure. For example, installing sliding or elastic supports can effectively release part of the temperature stress.

References

[1] D.S. Chen, W.C. Xu, H.L. Qian, et al., "Effects of non-uniform temperature on closure construction of spatial truss structure", *Journal of Building Engineering*, vol. 32, art. no. 101532, 2020, DOI: 10.1016/j.jobe.2020.101532.

[2] P. Woźniczka, "Fire Resistance Assessment of the Long-Span Steel Truss Girder", *Archives of Civil Engineering*, vol. 66, no. 2, pp. 63–75, 2020, DOI: 10.24425/ace.2020.131796.

[3] G. Flint, A. Usmani, S. Lamont, et al., "Effect of fire on composite long span truss floor systems", *Journal of Constructional Steel Research*, vol. 62, no. 4, pp. 303–315, 2006, DOI: 10.1016/j.jcsr.2005.08.002.

[4] R.K. Janardhan, et al., "Coupled CFD-FE analysis of a long-span truss beam exposed to spreading fires", *Engineering Structures*, vol. 259, art. no. 114150, 2022, DOI: 10.1016/j.engstruct.2022.114150.

[5] L. Lausova, I. Skotnicova, V. Michalcova, et al., "Effect of non-uniform temperature distribution over the cross-section in steel frame structure", *Applied Mechanics and Materials*, vol. 769, pp. 65–68, 2015, DOI: 10.4028/www.scientific.net/AMM.769.65.

[6] H. B. Liu, W. X. Liao, Z. H. Chen, et al., "Thermal behavior of spatial structures under solar irradiation", *Applied Thermal Engineering*, vol. 87, pp. 328–335, 2015, DOI: 10.1016/j.applthermaleng.2015.04.079.

[7] W.C. Xu, D.S. Chen, H.L. Qian, W. Chen, "Non-uniform temperature field and effects of large-span spatial truss structure under construction: Field monitoring and numerical analysis", *Structures*, vol. 29, pp. 416–426, 2021, DOI: 10.1016/j.istruc.2020.11.014.

[8] J. Liu, Y.S. Liu and G. Li, et al., "Temperature stress analysis and measures of large-span steel roof structure of National Exhibition and Convention Center in Shanghai", *Building Structure*, vol. 50, pp. 40–45, 2020, DOI: 10.19701/j.jzjg.2020.12.007 (in Chinese).

[9] C. Fan, Z. Wang, and J. Tang, "Analysis on temperature field and determination of temperature upon healing of large-span steel structure of the National Stadium", *Journal of Building Structures*, vol. 50, pp. 32–40, 2007, DOI: 10.14006/j.jzjgxb.2007.02.004 (in Chinese).

[10] B.B. Chen, "Study on Heterogeneous Temperature effect of large span structures under solar radiation", M.A. thesis, Tianjin University, China, 2014.

[11] F.C. Mcquiston, J.D. Parker, *Heating, ventilating, and air conditioning*. New York, USA: Springer US, 1989.

[12] Y. Chen, "Analysis and experimental study on the non-uniform solar temperature effect of steel tube structure", M.A. thesis, Harbin Institute of Technology, 2016.

[13] Y. Sun, Y.J. Guo, "Analysis of temperature-field and stress-field of steel plate concrete composite shear wall in early stage of construction", *Archives of Civil Engineering*, vol. 67, no. 1, pp. 351–366, 2021, DOI: 10.24425/ace.2021.136477.